Department of Thoracic Surgery, Institute of Surgery, Third Military Medical University[1]; Chongqing Key Laboratory of Biochemical & Molecular Pharmacology, Medicine Engineering Research Center, Chongqing Medical University[2], Chongqing PR China

Preparation and characterization of poly(lactic acid) nanoparticles for sustained release of pyridostigmine bromide

Q. Y. Tan[1,*], M. L. Xu[2,*], J. Y. Wu[2], H. F. Yin[2], J. Q. Zhang[2]

Received July 15, 2011, accepted August 28, 2011

Dr. Zhang Jingqing, Chongqing Key Laboratory of Biochemical & Molecular Pharmacology, Medicine Engineering Research Center, Chongqing Medical University, Rm 501, Building 22, Jingdi Garden, Daping, Yuzhong District, Chongqing 400042, PR China
zjqrae01@163.com

[*] *These authors contributed equally to this work.*

Pharmazie 67: 311–318 (2012) *doi: 10.1691/ph.2012.1103*

A novel pyridostigmine bromide poly (lactic acid) nanoparticles (PBPNPs) was prepared to obtain sustained release characteristics of PB. A central composite design approach was employed for process optimization. The *in vitro* release studies were carried out by dialysis method and conducted using four different dissolution media. Similar factor method was investigated for dissolution profile comparison. Multiple linear regression analysis for process optimization revealed that the optimal PBPNPs were obtained where the values of the amount of PB (X_1, mg), PLA concentration (X_2, % w:v), and PVA concentration (X_3, % w:v) were 49.20 mg, 3.31% and 3.41%, respectively. The average particle size and zeta potential of PBPNPs with the optimized formulation were 722.9 ± 4.3 nm, and -25.12 ± 1.2 mV, respectively. PBPNPs provided an initial burst of drug release followed by a very slow release over an extended period of time (72 h). Compared with free PB, PBPNPs had a significantly lower release rate of PB *in vitro*. The *in vitro* release profile of the PBPNPs could be described by Weibull models, regardless of type of dissolution medium. Statistical significance of similarity between every two dissolution profiles of PBPNPs in different dissolution media was found, and the difference between the curves of PBPNPs and pure PB was statistically significant.

1. Introduction

Pyridostigmine bromide (PB; $C_9H_{13}BrN_2O_2$; MW 261.12; Fig. 1), a quaternary ammonium compound, acts as a reversible inhibitor of cholinesterase. For more than 50 years PB has been used for the symptomatic treatment of myasthenia gravis and antagonism of nondepolarizing neuromuscular blockers. PB may also be used after abdominal surgery flatulence and urinary retention (Andersen et al. 2010; Maselli et al. 2011). PB is very soluble in water, which may be responsible for the short half-life (1∼2 h) and poor bioavailability in healthy volunteer (11.5%∼18.9%) (Breyer-Pfaff et al.1985; White et al. 1981). Mestinon® (pyridostigmine bromide tablets) is given orally and the treatment schedule with usually 5∼6 doses every day is recommended for adult patients. A sustained release drug delivery system is then required to avoid the need for frequent administration. The sustained release formulation on the market (Mestinon Timespan®, sustained release tablet) can be taken once or twice daily. The results of one recent non-interventional prospective open-label trial support the usefulness of the sustained-release dosage form of PB in an individualized therapeutic regimen to improve quality of life regardless of the patient's age in myasthenia gravis (Sieb et al. 2010). Other modified released dosage forms of PB (microparticles, pellets and HPMC-based sustained release tablet, etc.), with similar *in vitro* release characteristics of PB, have been developed and reported (Hegazy et al. 2002; Huang et al. 2007). For example, it was observed that the cumulative percentage of release from the microparticles prepared by solvation of PB reached 100% at the 3rd hour, while it reached 100% at the 12th hour from the PB microparticles prepared by dispersion of the active agent.

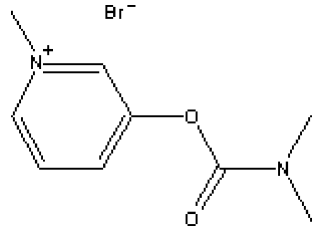

Fig. 1: Chemical structure of PB

To obtain an improvement of drug sustained release performance, other approaches such as nanoparticulate systems are rapidly developing in recent years (Adair et al. 2010). Especially, poly (lactic acid) (PLA) nanoparticles are getting more and more attention. Being a biodegradable polymer with Food and Drug Administration (FDA, United States) approval for human clinical use, PLA has been widely used in biomedical applications because of its good biocompatibility (Ishihara et al. 2010).

In the experiments outlined below, nanotechnology was employed to develop an alternative sustained release drug delivery system for PB, a synthetic drug with high solubility and

Table 1: Composition of central composite design batches (n = 3)

Batches	Factors			Y_1 (Entrapment efficiency, %)		Y_2 (Drug loading capacity, %)	
	X_1	X_2	X_3	Experimental	Predicted	Experimental	Predicted
1	−1	−1	−1	30.71	30.67	2.95	3.09
2	1	−1	−1	25.39	26.11	5.34	5.67
3	−1	1	−1	43.00	41.88	1.88	1.83
4	1	1	−1	32.34	34.81	3.13	3.25
5	−1	−1	1	32.41	30.52	3.09	3.16
6	1	−1	1	33.77	35.46	6.91	7.14
7	−1	1	1	48.00	47.86	2.09	1.95
8	1	1	1	49.66	50.28	4.73	4.77
9	−1.68	0	0	36.51	38.10	1.19	1.27
10	1.68	0	0	39.88	36.30	6.15	5.81
11	0	−1.68	0	25.03	26.25	6.31	5.94
12	0	1.68	0	47.73	48.15	2.79	2.90
13	0	0	−1.68	32.37	30.75	3.12	2.89
14	0	0	−1.68	44.22	43.64	4.25	4.22
15	0	0	0	37.03	37.20	3.39	3.53
16	0	0	0	37.03	37.20	3.54	3.53
17	0	0	0	37.37	37.20	3.57	3.53
18	0	0	0	37.12	37.20	3.54	3.53
19	0	0	0	37.24	37.20	3.55	3.53
20	0	0	0	37.12	37.20	3.54	3.53

poor oral bioavailability. This sustained release delivery system is expected to be administered by gastrointestinal or parenteral routes to gain much longer duration of action compared to that of free PB, PB sustained tablet on the market and other PB sustained formulations reported before. The objectives of this study are as follows: (1) PLA nanoparticles of PB (PBPNPs) was prepared by the double emulsion solvent evaporation method, and a circumscribed central composite design (CCD) approach was chosen to properly formulate PBPNPs (Liu et al. 2010; Basarkar et al. 2007). (2) The morphology of PBPNP was observed under optical microscopic. Moreover, the size distribution and zeta potential of PBPNPs were characterized by light scattering analysis. (3) The *in vitro* release behaviors of PBPNPs in deferent dissolution media were investigated by dialysis method in order to evaluate the sustained release characteristic of PBPNP in comparison to that of free PB.

This study was carried out to investigate the feasibility of preparing biodegradable PB nanoparticles using the double-emulsion solvent evaporation technique. The highly water soluble PB could very well be entrapped in the PLA nanoparticles and their characteristics could be monitored by making changes in various formulation and process variables.

In the present work, PBPNPs are prepared by the double emulsion solvent evaporation method, and the process optimization is performed using central composite design-response surface methodology. Our study confirmed that the values of the amount of PB, PLA concentration and PVA concentration had significantly impacts on the entrapment efficiency and drug-loading capacity of PBPNPs. PBPNPs prepared under the optimized protocol, being in nanometer range and good uniformity in size, had spherical shapes with smooth surfaces. *In vitro* dissolution tests in different dissolution media were performed to study the release properties of PBPNPs. Compared with free PB, PBPNPs had a significantly lower release rate of PB *in vitro*. Further studies are necessary to evaluate the *in vivo* release behavior and the *in vitro-in vivo* correlation. In a word, PBPNPs are very promising and need to be studied extensively which may ease the pressure of developing new acetylcholinesterase inhibitors.

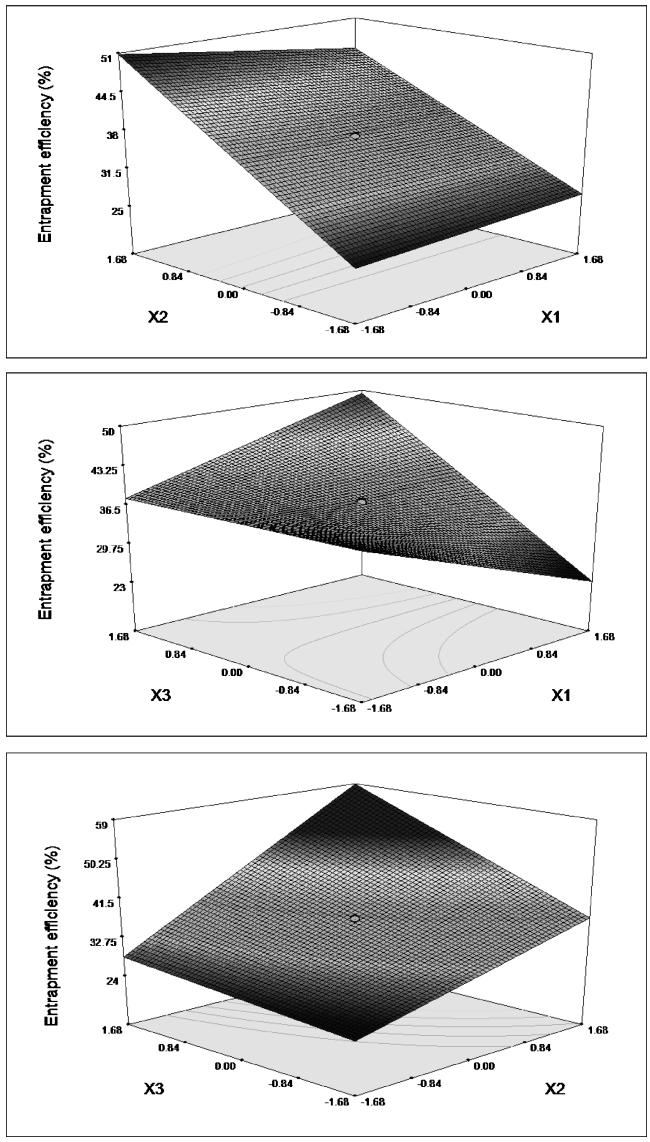

Fig. 2: Response surface plot showing the influence of the amount of PB (X_1, mg), PLA concentration (X_2, % w:v), and PVA concentration (X_3, % w:v) on entrapment efficiency (Y_1, %)

2. Investigations, results and discussion

2.1. Preparation of PBPNPs

The main constituents of PBPNPs, namely PLA as encapsulation materials and PVA as surfactant and spatially stable reagent, were tried in different concentrations to optimize the final formulation characteristics such as globule size range, polydispersity index, zeta potential, entrapment efficiency, drug loading capacity, structural integrity, and sustainability. However, the emphasis was given to the percent entrapment efficiency and drug loading capacity.

As depicted in Table 1, the entrapment efficiency (Y_1, 25.03% ∼ 49.66%) and drug loading capacity (Y_2, 1.19% ∼ 6.91%) for the 20 batches vary greatly. By applying multiple regression analysis on the experimental data, the following second-order polynomial equations are found to explain the PBPNPs production:

$$Y_1 = 31.45 - 4.49\,X_1 + 0.57\,X_2 - 7.99\,X_3 - 0.04\,X_1\,X_2 + 2.24\,X_1\,X_3 + 0.14\,X_2\,X_3 + 0.15\,X_{12} - (3.04E-3)\,X_2^2 + 0.31\,X_3^2 (r = 0.9829) \quad (1)$$

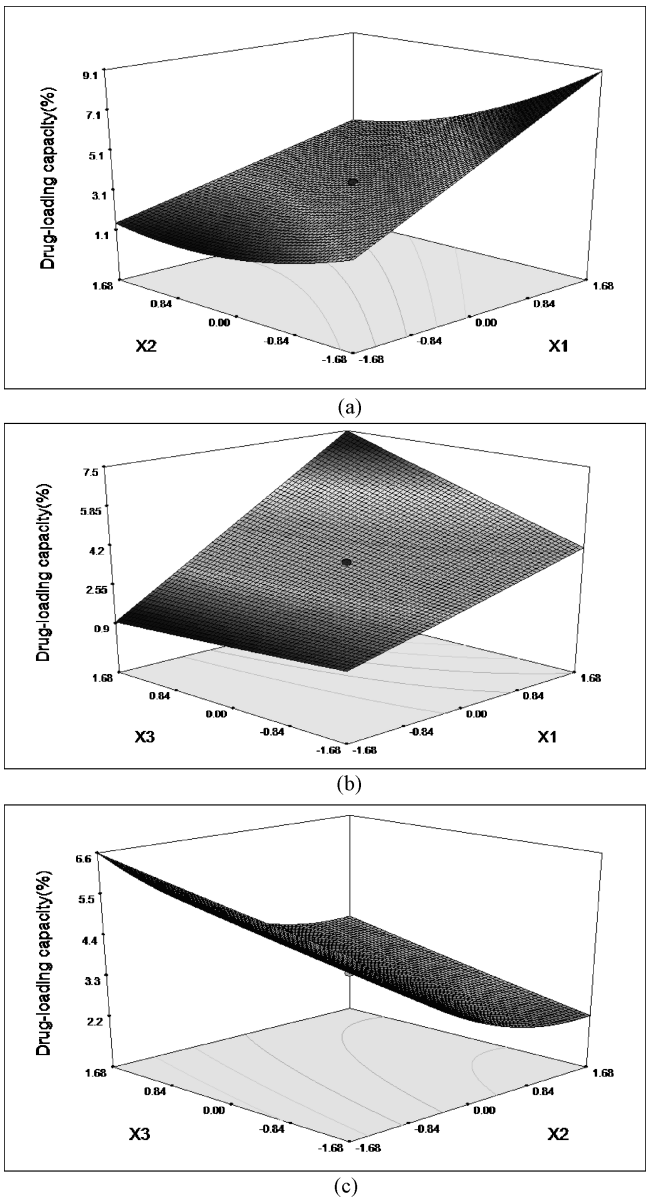

Fig. 3: Response surface plot showing the influence of the amount of PB (X_1, mg), PLA concentration (X_2, % w:v), and PVA concentration (X_3, % w:v) on drug loading capacity (Y_2, %)

$$Y_2 = 3.81 + 1.07\,X_1 - 0.15\,X_2 - 0.63\,X_3 - 0.22\,X_1\,X_2 + 0.33\,X_1\,X_3 + (1.18E-3)\,X_2X_3 + (2.70\,E-3)\,X_1{}^2 + 2.23\,X_2{}^2 + 0.01\,X_3{}^2 (r = 0.9932) \quad (2)$$

The results of *F* tests for ANOVA analysis indicate that both models described above are statistically significant ($P < 0.001$). In the case of entrapment efficiency (Y_1), the results presented in Table 2 indicate that the terms (X_2, X_3 and X_1 X_3) are statistically significant ($P < 0.01$). The interaction terms (X_2 X_3) are also statistically significant ($P < 0.05$). The linear and quadratic effects (X_2, $X_1{}^2$ and $X_3{}^2$) and the interaction terms (X_1 X_3 and X_2 X_3) have positive effects on the response variable, meaning that the entrapment efficiencies increase as these variables increase. The influence of main variables on entrapment efficiency decreases in the order of X_3, X_1, X_1 X_3, X_2 and $X_3{}^2$.

In the case of drug loading capacity (Y_2), The results presented in Table 3 indicate that the terms (X_1, X_2, X_3, X_1 X_2, X_1 X_3, and $X_2{}^2$) are statistically significant ($P < 0.01$). Moreover, the effects (X_1, X_1 X_3, X_2 X_3, $X_1{}^2$, $X_2{}^2$and $X_3{}^2$) have positive effects on the response variable, while the effects (X_2, X_3 and X_1 X_2) have negative effects on the response variable. The influence of main variables on drug loading capacity decreases in the order of $X_2{}^2$, X_1, X_3, X_1 X_3, and X_1 X_2.

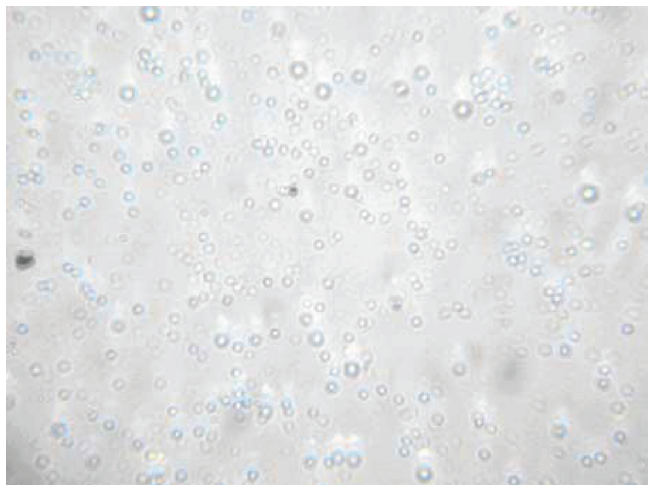

Fig. 4: Photomicrographs of PBPNPs (2000×)

The relationship between a response variable and a set of explanatory variables can be easily visualized by means of response surface methodology (Kouchakzadeh et al. 2010; Román-Velázquez et al. 2011). Response surface and contour plots were generated graphically using Design Experts 7.1.6 program (Version 7.1.6, Stat - Ease Inc., Minneapolis, USA). As depicted in Fig. 2 and Fig. 3, high levels of X_1 X_3, X_2 X_3, $X_1{}^2$, $X_3{}^2$and low levels of X_3, X_1 X_2 were found to be favorable condition for obtaining both high entrapment efficiency and drug loading capacity. In addition, high levels of X_2 and low levels of X_1, $X_2{}^2$ were found to be favorable condition for obtaining high entrapment efficiency; high levels of X_1, $X_2{}^2$ and low levels of X_2 were found to be favorable condition for obtaining high drug loading capacity, respectively. Above analysis suggests a complexelationship between variables and response (Martins et al. 2009).

Taken together, our findings suggest that the optimal values for the amount of PB (X_1, mg), PLA concentration (X_2, % w:v), and PVA concentration (X_3, % w:v) should be 49.20 mg, 3.31% (w:v) and 3.41% (w:v), respectively.

2.2. Validation of model optimization

In order to evaluate the optimization entrapment efficiency and drug loading capacity of the generated models obtained by central composite design, PBPNPs were prepared under the above described protocol (X_1, X_2 and X_3 were set to 49.20 mg, 3.31% and 3.41%, respectively). The entrapment efficiency and drug loading capacity obtained with predicted models are shown in Table 4, which is in good agreement on preparation properties

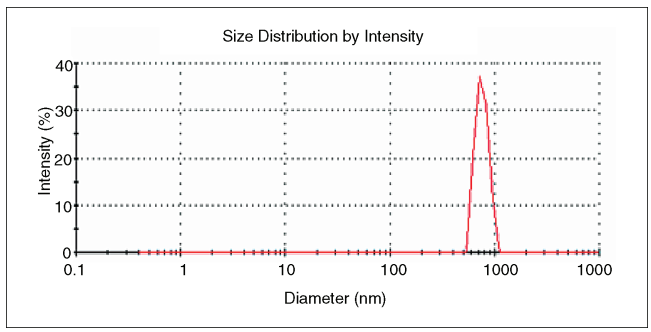

Fig. 5: Particle size distribution

Table 2: Statistical significance test for terms within the frame of generalized quadratic model in the case of entrapment efficiency (Y_1)

Source	X_1	X_2	X_3	$X_1 X_2$	$X_1 X_3$	$X_2 X_3$	X_1^2	X_2^2	X_3^2
Coefficient	−4.49	0.57	−7.99	−0.04	2.24	0.14	0.15	−(3.04E-3)	0.31
F value	31.58	1.29	192.40	1.06	15.00	6.23	0.22	0.88	0.29
P value	0.28	< 0.0001	< 0.0001	0.33	0.0031	0.032	0.65	0.37	0.60

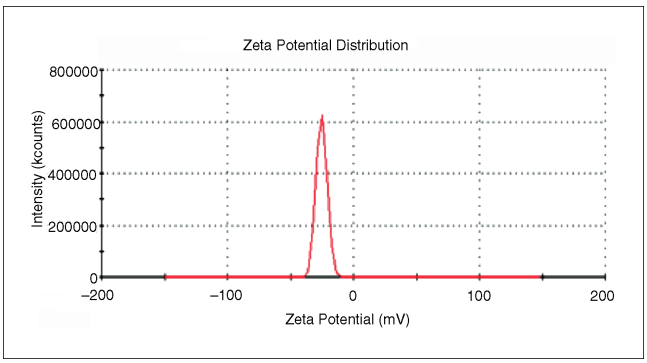

Fig. 6: Zeta potential

with theoretical predictions. The average entrapment efficiency and drug loading capacity of PB in PBPNPs prepared under the optimized conditions was found to be 51.98 ± 1.28% and 7.01 ± 0.31% (n = 3), respectively.

As far as PLA nanoparticles are concerned, the entrapment efficiencies were documented as 10%–23% (Musumeci et al. 2006), 45 ± 5% (Kumari et al. 2011), 65.3 ± 5.7% (Lan et al. 2011), 11.3%-38.3% (Kunii et al. 2011), 65.15% (Hou et al. 2011) and 2.6%-9.2% (Leo et al. 2004) in former research separately. In addition, there were a few reports of the drug loading capacity, which was recorded as 5.16% (Hou et al. 2011), 8% (Kumari et al. 2011), 0.64%–2.31% (Leo et al. 2004), and 0.14%–1.59% (Kunii et al. 2011). The change in the entrapment efficiency and drug loading capacity may be due to different type, amount, solubility properties of the drug used before, different preparation method and the object of study. The PBPNPs were designed and prepared to achieve good sustained release of PB in our experiments. The result of the experiment *in vitro* confirmed our assumption.

2.3. Characteristics of PBPNPs

As showed in Fig. 4, PBPNPs almost displayed spherical shape with smooth surface and no aggregation was observed. The size of the optimized formulation was 722.9 ± 4.3 nm with the polydispersity index of 0.095 ± 0.06 (Fig. 5). The nanometer range and a good uniformity in the PBPNPs size may be ascribed to the composition of the prepared nanoparticles in which the optimum level of PLA intercalates with that of surfactant (PVA) to provide the W1/O/W2 double emulsion with interfacial barrier of desired strength and efficiency. The zeta potential of the optimized formulation was - 25.12 ± 1.2 mV with the width of 2.1 ± 0.1 mV (Fig. 6). Zeta potential of nanoparticles was negative; it was due to the presence of terminal carboxylic groups in the polymers we used. The high potential value ensures a high-energy barrier stabilizing the nanosuspensions. That is to say, the charge repulsion provides an electrostatic potential barrier to PBPNPs and then these nanoparticles could be optimal for drug delivery (Tan et al. 2010a).

2.4. In vitro release rate studies

Release profiles were obtained by sampling of the release medium for up to 72 h and assayed spectrophotometrically for PB at 269 nm. Fig. 7 shows the drug release under changing pH values in four dissolution media: pH 7.4 PBS, 0.1 mol/L HCL, pH 6.8 PBS, and 0.1 mol/L HCl (2 h) and pH 6.8 PBS (70 h). Several mathematical models are used to fit the results, as shown in Table 5, which indicate that the Weibull model fits well, regardless of type of dissolution medium (Lu et al. 2003). PBPNPs provide an initial burst of drug release followed by a very slow release over an extended period of time (72 h). About 50% of the total PB in PBPNPs released in the first half an hour, which reflected the significant amount of unentrapped PB (Magenheim et al. 1993; Conte et al. 1995). In clinical practice, this would lead to "burst effect", which enables the preparation to show fast effect to the patients. On the other hand, the entrapped PB was prevented from diffusing into the dissolution medium by PLA nanoparticles, and this may be responsible for the slow release after 0.5 h. While for the free PB solution, under the same conditions, 85.44 ± 0.18% (n = 3) released in the first half an hour and 99.94 ± 0.01% (n = 3) in 24 h. The PB release rate of PBPNPs was found to be relatively low as compared to that of pure PB.

Among several methods investigated for dissolution profile comparison, similar factor (f_2) method is the simplest but reliable. So, f_2 method was investigated for dissolution profile comparison in our experiments. The f_2 value was calculated using the following formula

$$f_2 = 50lg\{\left[1 + (1/n)\sum_{i=1}^{n} W_t\left(\overline{X_{ii}} - \overrightarrow{X_{ri}}\right)^2\right]^{-1/2} \times 100\} \quad (3)$$

Where f_2 is the similar factor, $\overline{X_{ii}}$ and $\overrightarrow{X_{ri}}$ are drug cumulative release at time t of the two dissolution profiles, respectively, n

Table 3: Statistical significance test for terms within the frame of generalized quadratic model in the case of drug loading capacity (Y_2)

Source	X_1	X_2	X_3	$X_1 X_2$	$X_1 X_3$	$X_2 X_3$	X_1^2	X_2^2	X_3^2
Coefficient	1.07	−0.15	−0.63	−0.22	0.33	1.18E-3	2.70E-3	2.23	0.01
F value	440.36	198.44	38.04	11.90	17.58	0.022	3.71E-3	25.28	0.021
P value	< 0.0001	< 0.0001	0.0001	0.0062	0.0019	0.88	0.95	0.0005	0.89

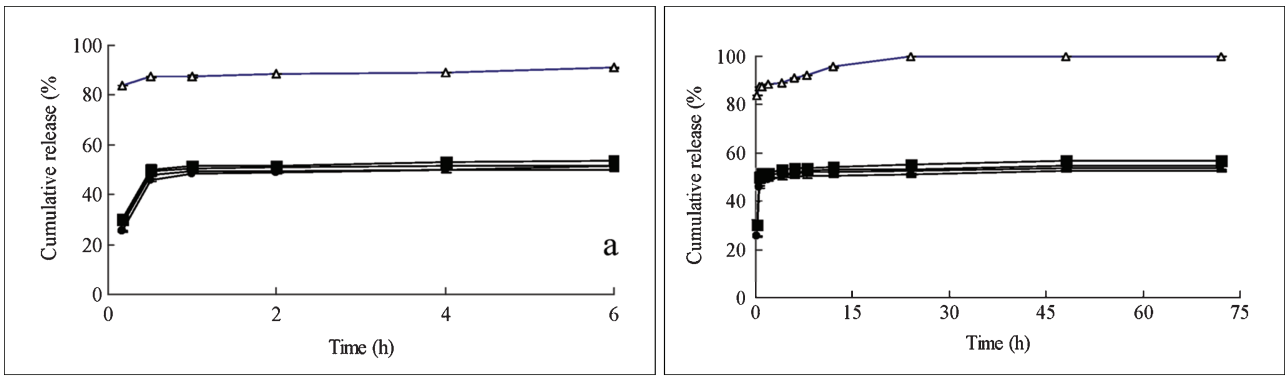

(a) (b)

Fig. 7: Drug release profiles of pure PB in the dissolution medium (pH 7.4 PBS, open triangles), and PBPNPs in four dissolution media (pH 7.4 PBS, closed triangles; 0.1mol/L HCL, closed cycles; pH 6.8 PBS, closed squares; 0.1 mol/L HCl for 2 h and subsequently at pH 6.8 PBS for 70 h, closed diamonds)

is the number of sampling point, W_t is the weight and set as 1 here.

When the two profiles are identical, the f_2 value is equal to 100. An average difference of 10% at all measured time point results in a f_2 value of 50. Food and Drug Administration (United States) has set a public standard of f_2 value (50–100) to indicate similarity between two dissolution profiles. The higher the value of similar factor the closer the similarity. As shown in Table 6 , statistical significance of similarity between every two dissolution profiles of PBPNPs in different dissolution media is found. On the other hand, there is significant difference between two curves when the f_2 value is below 50. As shown in Table 7, the difference between the curves of PBPNPs and pure PB is statistically significant.

In all, these results confirmed that the release rate of a highly water soluble drug (PB) could be controlled by entrapping it into PLA nanoparticles. This suggested that the PBPNPs might be used as carriers for sustained release of PB in the therapy of myasthenia gravis.

3. Experimental

3.1. Materials

Pyridostigmine bromide (PB, purity 99.6%) was purchased from Yuancheng Technology Development Co., Ltd. (Wuhan, China). Polylactic acid (PLA, molecular weight 45,840–76,380) was supported by Research Center of Biomimetic Material Science and Engineering, Chongqing University (Chongqing, China). Polyvinyl alcohol (PVA-217) was obtained from Kuraray Co. Ltd. (Tokyo, Japan). All other chemical reagents were of analytical grade or better.

3.2. Preparation of PBPNPs

The PBPNPs were prepared by using a modified $W_1/O/W_2$ emulsion solvent-evaporation method (Chaisria et al. 2009; Musumeci et al. 2006). Briefly, 49.20 mg of PB was dissolved in 1.0 mL of deionized water, and the drug solution was then slowly added to 10 mL dichloromethane containing 3.31% w/v PLA under magnetic stirring (about 3000 rpm) to yield a primary W_1/O emulsion. Next, the primary W_1/O emulsion was added to 100 mL of a 3.41% w/v PVA aqueous solution (W_2) in ice-water bath. The reaction proceeded under magnetic stirring for 30 min to form a homogeneous milky suspension ($W_1/O/W_2$ emulsion), and then the organic solvent was evaporated off with hypobaric drying method. The obtained colloidal suspension was adjusted to total 100 mL with cold deionized water.

Table 4: Model-predicted and observed values of entrapment efficiency and drug loading capacity of PBPNPs prepared according to the optimal parameters (mean ± S.D., n = 3)

Formulation characteristics	Predicted value	Observed value	Bias*(%)
Entrapment efficiency (%)	51.66	51.98 ± 1.28	−0.62
Drug loading capacity (%)	6.94	7.01 ± 0.31	−1.01

* Bias was calculated according to this equation: Bias (%) = (predicted value-observed value)/predicted value × 100%.

3.3. Determination of percent entrapment efficiency and drug loading capacity

The PB-containing PLA nanoparticle suspension was centrifuged at 12,000 g for 10 min to separate the unentrapped drug (Zhang et al. 2007). The supernatant was analyzed spectrophotometrically at 269 nm (UV-5130, Shimadzu, Kyoto, Japan). The empty nanoparticles served as blank reference during the course of study (Fig. 8). The absorptance spectra of PBPNP and blank reference clearly display considerable overlap; hence, the direct UV-visible spectrophotometric method is not suitable for determining the PB concentration (Rodenas et al.1995; El-Gindy et al. 2004). Fortunately, the second derivative spectra have spectral features that can be used for the determination (Fig. 9). Suitable settings were a slit width of 8 nm and a fast scan speed. The recorder scale expansion was optimized to facilitate reading on the recorder tracing. The PB amplitude was measured from baseline to positive peak at 287 nm, and the standard regression equation in the range of C = 16.68–38.92 μg/mL is linear (D = 0.0094 C + 0.0066, r = 0.9998, n = 3. D means the PB amplitude). The recoveries

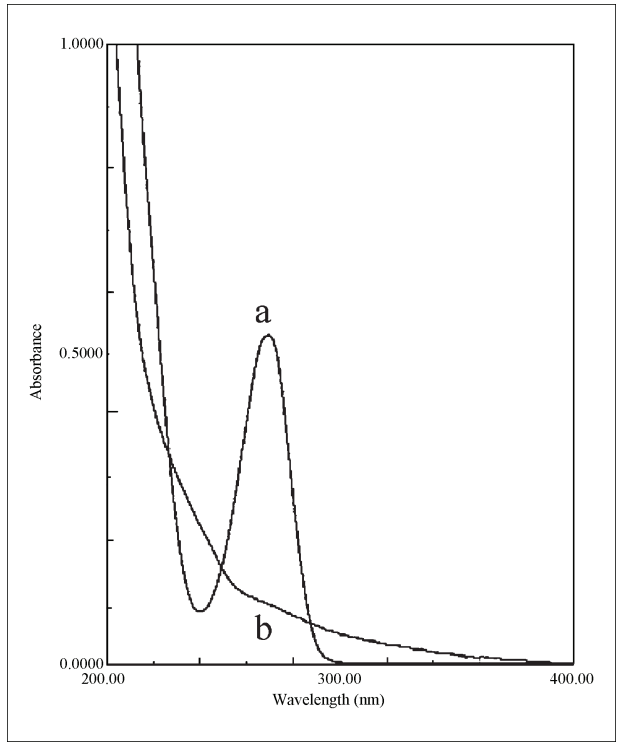

Fig. 8: Zero order spectra of (a) the supernatant of PBPNPs; (b) the supernatant of empty nanoparticles

Table 5: Mathematical models of mean cumulative release rate versus time

Release medium	Zero-order kinetic model	First-order kinetic model	Higuchi model	Weibull model
pH 7.4 PBS	$Q = 0.1119\ t + 51.897\ r = 0.8999$	$\ln(1\text{-}Q) = -0.0024\ t + 3.8734\ r = 0.9087$	$Q = 0.9205 t^{1/2} + 50.564\ r = 0.9603$	$\ln\ln[1/(1\text{-}\ Q)] = 0.0373\ t$ - 0.3363, $r = 0.9836$
0.1 mol/L HCl	$Q = 0.0305\ t + 51.897\ r = 0.8782$	$\ln(1\text{-}Q) = -0.0006\ t + 3.8862\ r = 0.8861$	$Q = 0.4163\ t^{1/2} + 50.353\ r = 0.9543$	$\ln\ln[1/(1\text{-}\ Q)] = 0.0258\ t$ - 0.3629 $r = 0.9908$
pH 6.8 PBS	$Q = 0.723\ t + 49.228\ r = 0.8905$	$\ln(1\text{-}Q) = -0.0015\ t + 3.9274\ r = 0.8976$	$Q = 0.5874\ t^{1/2} + 48.389\ r = 0.9394$	$\ln\ln[1/(1\text{-}\ Q)] = 0.0243\ t$ - 0.4042 $r = 0.9599$
0.1 mol L^{-1} HCL (2 h) and pH 6.8 PBS (70 h)	$Q = 0.1392\ t + 49.397\ r = 0.8019$	$\ln(1\text{-}Q) = -0.0029\ t + 3.9234\ r = 0.8149$	$Q = 1.2073\ t^{1/2} + 47.54\ r = 0.9026$	$\ln\ln[1/(1\text{-}\ Q)] = 0.0529\ t$ - 0.4254 $r = 0.9780$

Q means cumulative PB release at time t.

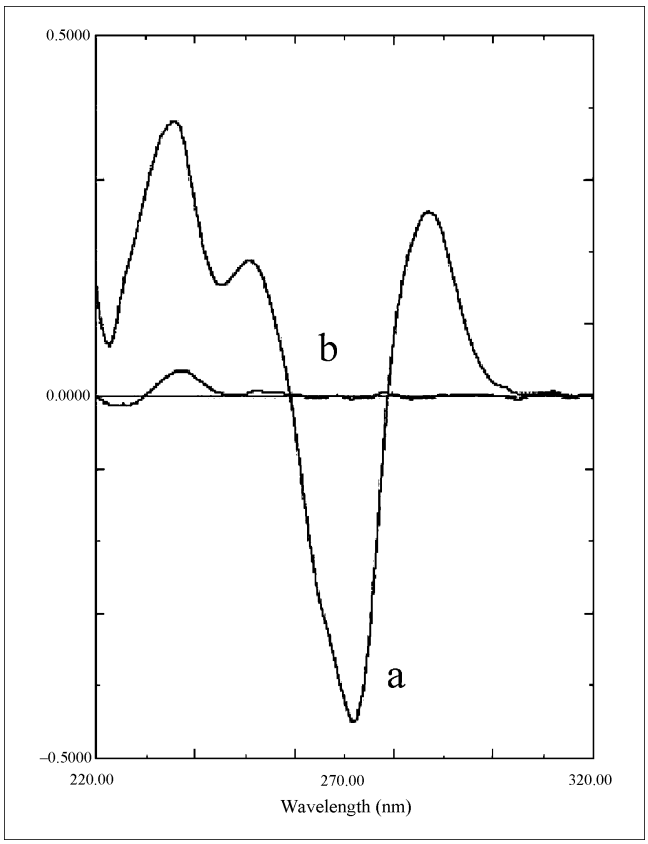

Fig. 9: Second order derivative spectra of (a) the supernatant of PBPNPs; (b) the supernatant of empty nanoparticles

of PB are 100.30 ± 0.94%(mean ± SD, n = 9), which showed that the above method was reliable for determination under the described conditions. Percentage entrapment efficiency (EE %) and drug-loading capacity (DL %) were calculated using the following formula (Zhang et al. 2005):

$$\text{EE}\ (\%) = \frac{\text{W}_{\text{total drug added}} - \text{W}_{\text{free drug}}}{\text{W}_{\text{total drug added}}} \times 100\% \quad (4)$$

$$\text{DL}\ (\%) = \frac{\text{W}_{\text{total drug added}} - \text{W}_{\text{free drug}}}{\text{W}_{\text{total drug added}} + \text{W}_{\text{total PLA added}}} \times 100\% \quad (5)$$

where "$W_{\text{total drug added}}$" were the mass of drug and PLA used for the preparation, respectively, "$W_{\text{free drug}}$" was the mass of free drug detected in the supernatant after centrifugation of the preparation.

3.4. Formulation component optimization

Various formulation factors were reported to have a key role on the entrapment efficiency and drug loading capacity of PLA nanoparticles (Liu et al. 2010; Nagarwal et al. 2010). Our preliminary experiment results revealed that the factors of the amount of PB (X_1, mg), PLA concentration (X_2, % w:v), and PVA concentration (X_3, % w:v) had relatively great influence on the entrapment efficiency and drug loading capacity. Thus, a three-factor, five-level central composite design (Gonzalez-Mira et al. 2011; Nevarez et al. 2010) was used to determine the optimal factors of preparation process for PBPNPs. The data was fitted to a quadratic model by Design Experts 7.1.6 program (Version 7.1.6, Stat - Ease Inc., Minneapolis, USA). This model was expressed as follows:

$$\begin{aligned} \text{Y}_\text{i} = {} & \beta_0 + \beta_1 \text{X}_1 + \beta_2 \text{X}_2 + \beta_3 \text{X}_3 + \beta_{12} \text{X}_1 \text{X}_2 + \beta_{13} \text{X}_1 \text{X}_3 \\ & + \beta_{23} \text{X}_2 \text{X}_3 + \beta_{11} \text{X}_{12} + \beta_1^2 \text{X}_{22} + \beta_{33} \text{X}_3^2 \end{aligned} \quad (6)$$

where Y_i is the dependent variable, Y_1 and Y_2 are the entrapment efficiency and drug loading capacity, respectively. β_0 is the intercept representing the arithmetic mean response of the twenty runs, and β_i is the estimated coefficients for the factor X_i. The main effects (X_1, X_2 and X_3) represent the average results of changing one factor at a time from its minimal to maximal value. The interaction terms (X_1X_2, X_2X_3 and X_1X_3) show how the response changes when two factors are simultaneously changed. The polynomial terms (X_1^2, X_2^2 and X_3^2) are included to investigate non-linearity. The levels of three independent variables and the composition of the central composite design batches are presented in Table 1 and Table 8.

3.5. Morphology and structure

Morphology and structure of PBPNPs were determined using biomicroscopy (XSP-35–1600X, Phoenix, Shangrao, China), and photomicrographs were taken at suitable magnifications by camera (C-60 ZOOM, Olympus, Hongkong, China). Before analysis, the nanoparticle dispersions were diluted 1:10 with distilled water.

3.6. Photon correlation spectroscopy and zeta potential

The average diameter and polydispersity index of PBPNPs were determined by photon correlation spectroscopy (Zeta-Sizer Nano-ZS90, Malvern, UK) at 25 °C. The zeta potential and width were performed with the same device. The PBPNP water dispersions were diluted 1:10 with distilled water before analysis. Each sample was analyzed in triplicate. The polydispersity index measures the size distribution of the nanoparticle population (Musumeci et al. 2006).

3.7. In vitro release rate studies

The studies were carried out by a modified dialysis method (Tan et al. 2010b). Briefly, the PBPNPs contained 10 mg of PB were filled in dialysis bags and soaked in diffusion medium of 150 mL conic flask. The study was run at 100 rpm, and the dissolution vessel was maintained at 37 ± 0.5 °C. An aliquot sample of 0.5 mL was withdrawn at designated time intervals. The dissolution medium was then replaced by 0.5 mL of fresh dissolution fluid to maintain a constant volume. The quantitative determination of the drug was carried out using second derivative spectrophotometry, and the mean cumulative release rate was then calculated. The procedures were applied to the three batches of PBPNPs and pure PB. The *in vitro* release studies

Table 6: Similarity between the dissolution profiles of PB and PBPNPs in different dissolution media

Released medium	f_2
0.1mol/L HCL	19.21
pH 7.4 PBS	20.06
pH 6.8 PBS	18.43
0.1 mol L^{-1} HCL (2 h) and pH 6.8 PBS (70 h)	18.72

Table 7: Similarity between every two dissolution profiles of PBPNPs in different dissolution media

Released medium 1	Released medium 2	f_2
0.1mol/L HCL	pH 7.4 PBS	84.67
0.1mol/L HCL	pH 6.8 PBS	87.09
0.1mol/L HCL	0.1 mol/L HCl (2 h) and pH 6.8 PBS (70 h)	82.19
pH 7.4 PBS	pH 6.8 PBS	73.95
pH 7.4 PBS	0.1 mol/L HCl (2 h) and pH 6.8 PBS (70 h)	76.38
pH 6.8 PBS	0.1 mol/L HCl (2 h) and pH 6.8 PBS (70 h)	83.34

Table 8: Coded levels and "real" values for each factor under study

Factors	Levels				
	–1.68	–1	0	1	1.68
X_1 (PB, mg)	10	18.11	30	41.89	50
X_2 (PLA, % w/v)	1	1.81	3	4.19	5
X_3 (PVA, % w/v)	0.5	1.11	2	2.89	3.5

were conducted using four different dissolution media: (1) pH 7.4 phosphate buffer (PBS); (2) 0.1 mol/L HCl; (3) pH 6.8 PBS; (4) 0.1mol/L HCl for the first 2 h, followed by pH 6.8 PBS (2 h later).

Acknowledgements: The authors wish to thank National Natural Science Foundation of China (No. 30973645), Chongqing Natural Science Foundation (No. CSCT2012JJB10019), and Specialized Research Fund for the Doctoral Program of Higher Education (No. 20095503120008).

References

Adair JH, Parette MP, Altinoğlu EI, Kester M (2010) Nanoparticulate alternatives for drug delivery. ACS Nano 4: 4967–4970.

Andersen JB, Engeland A, Owe JF, Gilhus NE (2010) Myasthenia gravis requiring pyridostigmine treatment in a national population cohort. Eur J Neurol 17: 1445–1450.

Basarkar A, Devineni D, Palaniappan R, Singh J (2007) Preparation, characterization, cytotoxicity and transfection efficiency of poly(DL-lactide-co-glycolide) and poly(DL-lactic acid) cationic nanoparticles for controlled delivery of plasmid DNA. Int J Pharm 343: 247–254.

Breyer-Pfaff U, Maier U, Brinkmann AM, Schumm F (1985) Pyridostigmine kinetics in healthy subjects and patients with myasthenia gravis. Clin Pharmacol Ther 37: 495–501.

Chaisria W, Hennink WE, Okonogi S (2009) Preparation and characterization of cephalexin loaded PLGA microspheres. Curr Drug Deliv 6: 69–75.

Conte U, Genta I, Giunchedi P, Modena T (1995) Testing of '*in vitro*' dissolution behaviour of microparticulate drug delivery systems. Drug Dev Ind Pharm 21: 1223–1233.

El-Gindy A, Emara S, Hadad GM (2004) Determination of certain drugs in binary mixtures formulations by second derivative ratio spectrophotometry and LC. Farmaco 59: 703–712.

Gonzalez-Mira E, Egea MA, Souto EB, Calpena AC, García ML (2011) Optimizing flurbiprofen-loaded NLC by central composite factorial design for ocular delivery. Nanotechnology 22: 045101.

Hegazy N, Demirel M, Yazan Y (2002) Preparation and *in vitro* evaluation of pyridostigmine bromide microparticles. Int J Pharm 242: 171–174.

Hou ZQ, Zhou CX, Luo Y, Zhan CM, Wang YX, Xie LY, Zhang QQ (2011) PLA nanoparticles loaded with an active lactone form of hydroxycamptothecin: development, optimization,and *in vitro–in vivo* evaluation in mice bearing h22 solid tumor. Drug Dev Res 72: 1–9.

Huang YT, Tsai TR, Cheng CJ, Cham TM, Lai TF, Chuo WH (2007) Formulation design of an HPMC-based sustained release tablet for pyridostigmine bromide as a highly hygroscopic model drug and its *in vivo/in vitro* dissolution properties. Drug Dev Ind Pharm 33: 1183–1191.

Ishihara T, Takahashi M, Higaki M, Mizushima Y, Mizushima T (2010) Preparation and characterization of a nanoparticulate formulation composed of PEG-PLA and PLA as anti-inflammatory agents. Int J Pharm 385: 170–175.

Kouchakzadeh H, Shojaosadati SA, Maghsoudi A, Vasheghani FE (2010) Optimization of PEGylation conditions for BSA nanoparticles using response surface methodology. AAPS PharmSciTech 11: 1206–1211.

Kumari A, Yadav SK, Pakade YB, Kumar V, Singh B, Chaudhary A, Yadav SC (2011) Nanoencapsulation and characterization of Albizia chinensis isolated antioxidant quercitrin on PLA nanoparticles. Colloids Surf B Biointerfaces. 82: 224–232.

Kunii R, Onishi H, Machida Y. (2007) Preparation and antitumor characteristics of PLA/(PEG-PPG-PEG) nanoparticles loaded with camptothecin. Eur J Pharm Biopharm 67: 9–17.

Lan CH, Rémi F, Yves W (2011) Increase in stability and change in supramolecular structure of b-carotene through encapsulation into polylactic acid nanoparticles. Food Chem 124: 42–49.

Leo E, Brina B, Forni F, Vandelli MA (2004) *In vitro* evaluation of PLA nanoparticles containing a lipophilic drug in water-soluble or insoluble form. Int J Pharm 278: 133–41.

Liu J, Qiu Z, Wang S, Zhou L, Zhang S (2010) A modified double-emulsion method for the preparation of daunorubicin-loaded polymeric nanoparticle with enhanced *in vitro* anti-tumor activity. Biomed Mater 5: 065002.

Lu B, Zhang JQ Yang H (2003) Non phospholipid vesicles of carboplatin for lung targeting. Drug Deliver 10: 87–94.

Magenheim B, Levy MY, Benita S (1993) A new *in vitro* technique for evaluation of drug release profile from colloidal carriers-ultrafiltration technique at low pressure. Int J Pharm 94: 115–123.

Martins SAM, Prazeres DMF, Fonseca LP, Monteiro GA (2009) Application of central composite design for DNA hybridization onto magnetic microparticles. Anal BioChem 391: 17–23.

Maselli RA, Henderson JD, Ng J, Follette D, Graves G. Wilson BW (2011) Protection of human muscle acetylcholinesterase from soman by pyridostigmine bromide. Muscle Nerve. 43: 591–595.

Musumeci T, Ventura CA, Giannone L, Ruozi B, Montenegro L, Pignatello R, Puglisi G (2006) PLA/PLGA nanoparticles for sustained release of docetaxel. Int J Pharm 325: 172–179.

Nagarwal RC, Singh PN, Kant S, Maiti P, Pandit JK (2010) Chitosan coated PLA nanoparticles for ophthalmic delivery: characterization, in-vitro and in-vivo study in rabbit eye. J Biomed Nanotechnol 6: 648–657.

Nevarez L, Vasseur V, Debaets S, Barbier G (2010) Use of response surface methodology to optimise environmental stress conditions on Penicillium glabrum, a food spoilage mould. Fungal Biol 114: 490–497.

Rodenas V, Parra A, Garcia-Villanova J, Gomez MD (1995) Simultaneous determination of cefepime and L-arginine in injections by second-derivative spectrophotometry. J Pharm Biomed Anal 13: 1095–1099.

Román-Velázquez, CE, Noguez, C (2011) Designing the plasmonic response of shell nanoparticles: spectral representation. J Chem Phys 134: 044116.

Sieb JP, Köhler W (2010) Benefits from sustained-release pyridostigmine bromide in myasthenia gravis: Results of a prospective multicenter open-label trial. Clin Neurol Neurosurg 112: 781–784.

Tan QY, Wang N, Yang H, Chen L, Xiong HR, Zhang LK, Liu J, Zhao CJ, Zhang JQ (2010a) Preparation and characterization of lipid vesicles containing uricase. Drug Deliver 17: 28–37.

Tan QY, Wang N, Yang H, Zhang LK, Liu S, Chen L, Liu J, Zhang L, Hu NN, Zhao CJ, Zhang JQ (2010b) Characterization, stabilization and activity of uricase loaded in lipid vesicles. Int J Pharm 384: 165–172.

White MC, De Silva P, Havard CW (1981) Plasma pyridostigmine levels in myasthenia gravis. Neurology 31: 145–150.

Zhang JQ, Liu J, Li XL, Jasti BR (2007) Preparation and characterization of solid lipid nanoparticles containing silibinin. Drug Deliv 14: 381–387.

Zhang JQ, Zhang ZR, Yang H, Tan QY, Qing SR, Qiu XL (2005) Lyophilized paclitaxel magnetoliposomes as a potential drug delivery system for breast carcinoma via parenteral administration: *in vitro* and *in vivo* studies. Pharm Res 22: 573–583.